Capillary Forces between Spheres during Agglomeration and Liquid Phase Sintering

K. S. HWANG, R. M. GERMAN, and F. V. LENEL

The capillary force due to a wetting liquid between solid particles is responsible for agglomeration and the rearrangement stage of liquid phase sintering. The capillary force has been calculated for several situations using a numerical technique. Included in the calculations are variations in particle size, contact angle, liquid volume, and particle separation. The capillary force obtained from these calculations is more accurate than prior estimates using a circular profile for the interparticle liquid bridge. A large attractive force exists between particles with small contact angles, particle sizes, and liquid volumes. Rupture of the liquid bridge is predicted using an energy analysis. At large contact angles, a zero force condition exists at an intermediate particle separation.

I. INTRODUCTION

IN liquid phase sintering and powder agglomeration, the system consists of solid particles, pores, and a liquid. In the initial stage of liquid phase sintering the solid particles often preserve their initial size and shape while undergoing rearrangement without significant dissolution of the solid in the liquid.[1] Likewise, in agglomeration processes such as spray drying a wetting liquid is used to pull particles into a dense cluster. An important parameter necessary to mathematically treat these processes is the capillary force existing between the solid particles and the liquid. The first step in calculating the capillary force is to consider a system consisting of two solid spherical particles connected by a liquid bridge. Even though such a system appears to be simple, the task of calculating the force may become quite formidable. The reason is that the capillary force depends on the shape of the liquid bridge which is a function of the contact angle, particle size, and amount of liquid. The true configuration of the bridge is called a nodoid and is described by a differential equation given below.

II. BACKGROUND

The capillary force F between two solid bodies connected by a liquid bridge depends on the shape of the liquid; an accurate description of the liquid profile is therefore desirable. In Figure 1, two spheres with radius A are shown separated by the distance D. The angle α is the semi-angle subtended by the perimeter where the solid, liquid, and vapor phases meet. The angle between the liquid-vapor surface tension vector γ_{l-v} and the x-axis is ϕ. The contact angle between the solid and the liquid is θ. The radius of curvature of the liquid surface in the x-y plane is S and its radius in the orthogonal plane is T. The equations describing these two radii are given by[2]

$$S = [1 + (y')^2]^{3/2}/y'' \qquad [1]$$

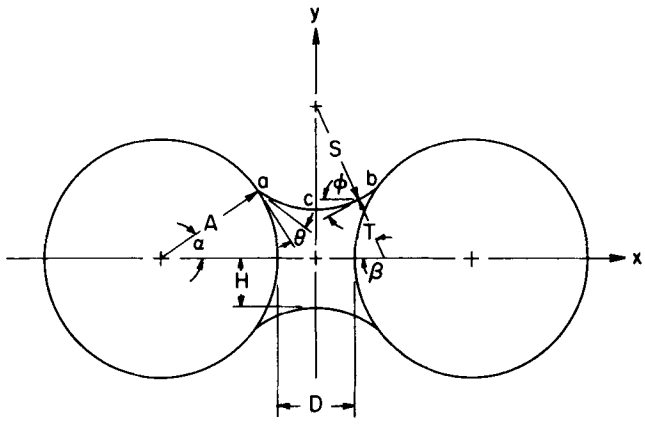

Fig. 1 — The geometry and definition of variables of a nodoid liquid profile which connects two identical spheres.

and

$$T = y/\sin\beta = y[1 + (y')^2]^{1/2} \qquad [2]$$

where y describes the liquid profile as a function of x, y' designates dy/dx, y'' designates d^2y/dx^2, and β is given in Figure 1.

Due to the curvature of the liquid-vapor interface, there will be a pressure differential P between the liquid meniscus and the vapor phase. According to the Laplace equation, the pressure deficiency of the liquid (neglecting the gravity effect) is given by

$$\gamma_{l-v}\left(\frac{1}{S} - \frac{1}{T}\right) = P. \qquad [3]$$

Substituting Eqs. [1] and [2] into Eq. [3] gives

$$P/\gamma_{l-v} = y''/[1 + (y')^2]^{3/2} - 1/[y(1 + (y')^2)]^{1/2}. \qquad [4]$$

Since the pressure is equal everywhere in the liquid, the pressure deficiency P in Eq. [4] is a constant. Equation [4] is thus a differential equation describing the profile of the liquid-vapor interface, the nodoid. This equation is general and applies to the liquid shown in Figure 1 as well as the case where the spheres are in contact ($D = 0$).

After the profile of the liquid bridge is found, the force between the spheres can be calculated by the force

K. S. HWANG is Materials Engineering Manager, Power Semiconductor Division, General Instrument Corporation, 600 West John Street, Hicksville, NY 11802. R. M. GERMAN and F. V. LENEL are Professors, Materials Engineering Department, Rensselaer Polytechnic Institute, Troy, NY 12180-3590.

Manuscript submitted July 7, 1986.

equation[3-10]

$$F = \pi y^2 P + 2\pi y \gamma_{l-v} \cos \phi . \quad [5]$$

The first term, $\pi y^2 P$, is due to the pressure deficiency in the liquid acting on the area of any cross section of the liquid bridge which is perpendicular to the x-axis. The second term, $2\pi y \gamma_{l-v} \cos \phi$, is due to the surface tension acting along the contact perimeter of that cross section of the liquid. The capillary force caused by this surface tension is then its projection onto the x-axis. Equation [5] is general. It can be applied to any point along the liquid-vapor interface.

Graphical, analytical, and numerical solutions to the capillary force problem have been supplied for a few specific cases[3,4,6,11-15] where the contact angles, particle sizes, and distances between particles are specific. In this study, we have further extended the solutions to the general case where spheres of different radii are either in point contact or are separated by a distance, and have included variable contact angles and liquid quantities.

III. CALCULATION METHODS

When gravity is neglected, the differential Eq. [4] defines the profile of the liquid and must be solved first in order to evaluate the capillary force. Gravity can be neglected for particles since the gravitational force is typically a very small fraction (10^{-4} to 10^{-5} for 100 μm particles) of the capillary force.[16] In Figure 2, two spheres with radii A_s and A_l are separated by a distance D. The liquid-vapor interface intercepts both spheres with a contact angle θ. The boundary conditions of Eq. [4] in such a system is that the contact angle must be maintained at points "a" and "b"

$$\text{at} \quad x = x_a \qquad y' = \tan(\pi/2 + \alpha_s + \theta) \quad [6]$$

$$\text{at} \quad x = x_b \qquad y' = \tan(\pi/2 - \alpha_l + \theta) \quad [7]$$

where α_s and α_l are the semi-angles subtended by the liquid bridge to the centers of the small and large particles, respectively (Figure 2).

Equation [4] and boundary conditions [6] and [7] completely specify the mathematical problem. The numerical procedure to solve this problem for a given combination of liquid volume, contact angle, particle sizes, and interparticle distance is described by Hwang.[16] After the profile of the liquid-vapor interface is found, the capillary force can be calculated from Eq. [5]. Based on the above procedure, computer programs were written to calculate the configuration and capillary force; listings of these programs are also given in the thesis by Hwang.

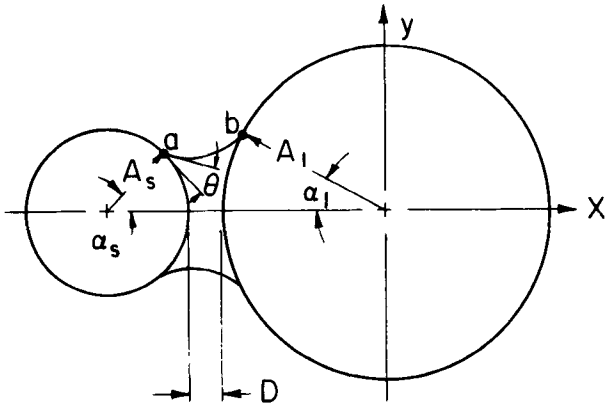

Fig. 2—The geometry and definition of variables of a nodoid liquid profile which connects two unequal sized spheres.

IV. RESULTS

The capillary force depends on the shape of the liquid bridge, which depends on the following main variables: (i) the contact angle θ measured between the solid-liquid and the liquid-vapor interface; (ii) A_l and A_s, the radius of the large and small spheres; these radii are also represented by a size ratio variable C which is defined as A_l/A_s (where A_l is greater than A_s so that C is greater than 1); (iii) the interparticle distance D; and (iv) V_{liq}, the absolute volume of the liquid bridge. Since the absolute value of the liquid volume depends on the scale of the system, we use a normalized liquid volume which is defined by

$$V = 3V_{liq}/4\pi A_s^3 . \quad [8]$$

The capillary force is a function of the above variables and can be represented using a normalized force F_n. The normalized force is defined as the ratio of the capillary force divided by the surface tension of the liquid and the radius of the small sphere,

$$F_n = \frac{F}{(\gamma_{l-v} A_s)} . \quad [9]$$

Since the computer program developed for studying the liquid profile and capillary force can produce extensive results, only the results of the calculations for specific combinations of contact angle, interparticle distance, liquid volume, and particle size ratio are presented. The size ratios C are 1, 5 and ∞ (the latter corresponding to a sphere and a plate); contact angles are 0 deg, 45 deg, and 85 deg; interparticle distances are from 0 to $0.2A_s$ (where A_s is the radius of the small particle); and normalized liquid volumes are 0.01 and 0.1. These liquid volumes are for one contact point; thus, they are realistic considering the multiple contact points between particles in a typical powder compact.

The capillary force results for various conditions will be divided between cases of small and large contact angles. There is a fundamental difference between these two cases. For small contact angles the capillary forces decrease with increasing distance D between the spheres but they remain attractive even for large distances. Nevertheless, even with attractive forces at these small contact angles, the configuration consisting of two spheres connected by a liquid bridge will become unstable at large interparticle distances and rupture will occur. On the other hand, for very large contact angles the capillary forces are repulsive for small distances between particles. As the distance increases the curves for capillary force pass through zero and become attractive for large separations.

A. *Low Contact Angles*

Families of curves of capillary forces for various conditions are shown in Figure 3 when the contact angle equals 0 deg. These curves show that with a zero contact angle the

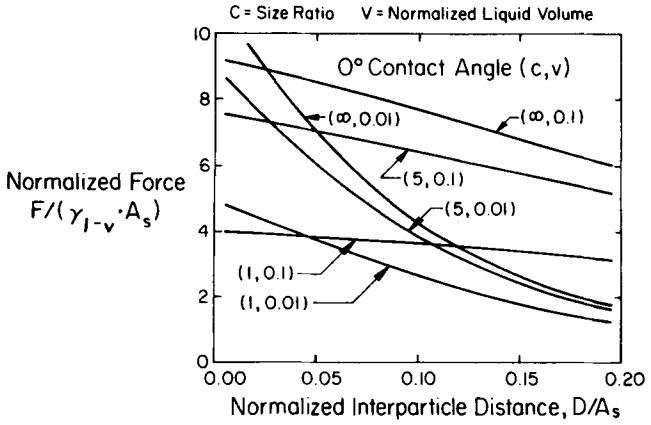

Fig. 3—The capillary force acting between two spheres or a sphere and a plate connected by a liquid bridge as a function of the normalized interparticle distance for a contact angle $\theta = 0$ deg, and particle size ratios $C = 1$, 5, and ∞.

capillary force between two spheres is positive (attractive), and its magnitude depends on the interparticle distance D, liquid volume V, and size ratio of particles C. The attractive force indicates that particle contact with $D = 0$ is preferred with wetting liquid bridges. For small values of D, the capillary force increases with decreasing values of liquid volume. This dependence can be seen by comparing the curve (1, 0.01) with curve (1, 0.1) and curve (5, 0.01) with (5, 0.1) near $D = 0$, where the first number denotes the size ratio C and the second number denotes the normalized liquid volume V.

Next, consider the effect of the particle size ratio on the capillary force. It is seen in Figure 3 that the normalized capillary force depends on the size ratio C. Comparing the curve (1, 0.1) with (5, 0.1) and (∞, 0.1) or the curve (1, 0.01) with (5, 0.01) and (∞, 0.01), it is seen that the normalized capillary force increases with increasing size ratio.

This dependence is based on the type of normalization of liquid volume V used in these results. With a different normalization of liquid volume, the influence of the size ratio on the capillary force will appear different. An example of the dependence of the capillary force on the size ratio based on the volume of both spheres is shown in Figure 4. (Note that the sphere-plate combination can not be shown using this format.) At a small interparticle distance D the capillary force for identical spheres ($C = 1$) is slightly smaller than for spheres with a size ratio of 5. As D increases, the difference of the capillary force between the two case becomes larger rather than smaller as in the case shown in Figure 3.

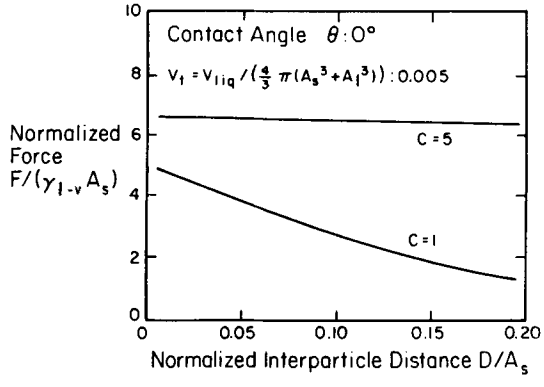

Fig. 4—The capillary force acting between two spheres connected by a liquid bridge as a function of interparticle distance for a contact angle $\theta = 0$ deg, particle size ratios $C = 1$ and 5, and with the liquid volume normalized by the total solid volume.

When D is small the capillary force increases with decreasing liquid volume and decreasing particle size uniformity. Therefore, when a strong capillary force is needed for a system consisting of spheres separated by a small distance, the liquid should be uniformly distributed so that the amount of liquid at each contact point is small. In addition, benefit may be gained by a wide particle size distribution.

As shown in Figure 3 for $\theta = 0$ deg, even though the normalized capillary force decreases with interparticle distance D, it nevertheless stays attractive in the range of D studied. It has often been assumed[17,18] that permanent separation of the two spheres (liquid rupture) will occur when the interparticle distance is very large because the capillary force passes through zero and becomes repulsive for large D. This is not correct. Configurations which consist of two spheres each of them with a cap of liquid, as shown in Figure 5, can have a lower free energy than when the liquid forms a bridge with a nodoid profile between the two spheres. Under this condition rupture of the bridge is expected.

Rupture can be explored by comparing the surface energy of a system consisting of two spheres connected by a bridge with a nodoid profile and the surface energy of two spheres with liquid caps. As shown in Figure 5, each of the caps is part of a sphere because the surface energy in that condition is at its minimum. In Figure 6 the difference in surface energy for the two configurations (nodoid and spherical caps) is plotted as a function of the interparticle distance for various liquid volumes. Rupture is expected when the energy difference is negative. This approach does not include the energy difference associated with the two different liquid pressure states. Since the pressure is higher in the spherical caps, inclusion of this factor will shift the rupture point to larger interparticle distances.

The values of interparticle distance at a given liquid volume when the surface energy difference is zero is shown in Figure 7 as a plot of capillary force *vs* interparticle distance. The points where the energy difference between the two configurations is zero is marked by circles and it is noted that the capillary forces at these points are still attractive.

Experimentally, the rupture phenomenon described above has been observed by Mason and Clark.[19] Their data are the

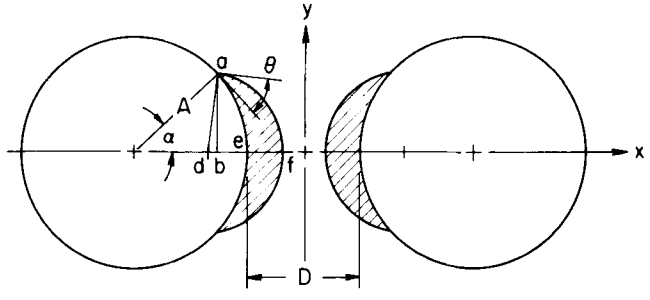

Fig. 5—The geometry and definition of variables of the liquid cap adhered to a sphere.

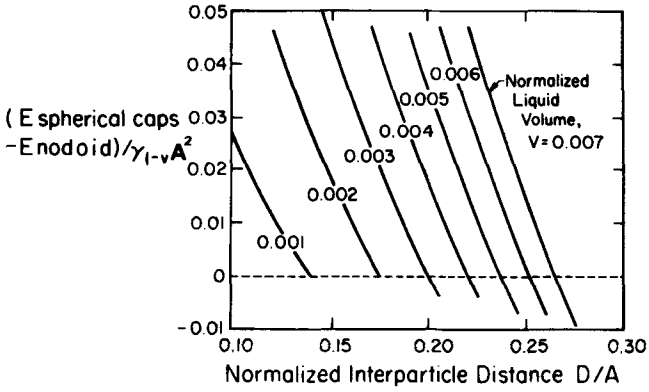

Fig. 6—Surface energy difference between a nodoid liquid bridge and spherical liquid caps in an identical spheres system.

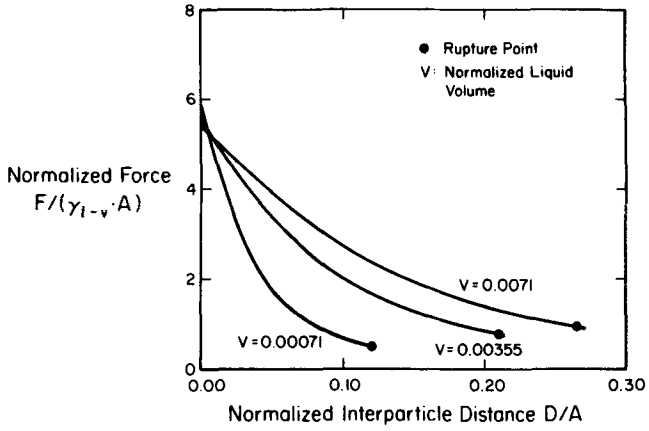

Fig. 7—The rupture point and the capillary force acting between two equal sized spheres connected by a liquid bridge as a function of the normalized interparticle distance for a contact angle θ = 0 deg.

points plotted in Figure 8. Also shown are the distances for different liquid volumes when rupture should occur on the basis of equal configurational energies. The predicted interparticle distances for rupture are somewhat smaller than those measured experimentally. This is expected since the capillary force at the critical rupture distance is still attractive as shown in Figure 7, and the energy associated with differences in liquid pressure is not included. Also, from thermodynamics, for a spontaneous process such as rupture

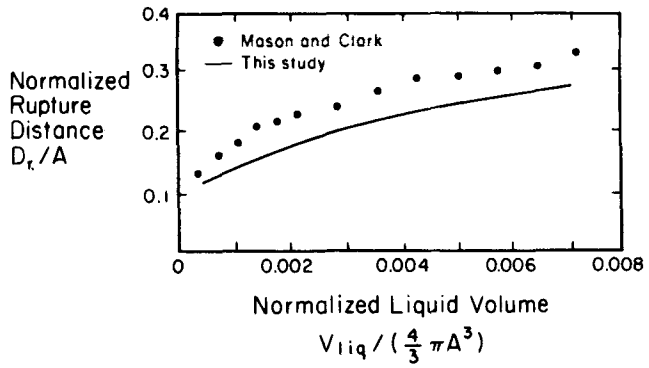

Fig. 8—A comparison between the calculation and the experimental data for the variation of bridge rupture distance with various liquid volumes for two identical spheres (C = 1) with a contact angle θ = 0 deg.

to occur, the free energy after rupture must be smaller than before. The measured rupture distances therefore should be larger than the values predicted for equal surface energies.

B. *Large Contact Angles*

In order to study how the contact angle θ affects the capillary force, the data in Figure 3 (θ = 0 deg), Figure 9 (θ = 45 deg), and Figure 10 (θ = 85 deg) should be compared. The data in Figure 9, in which the capillary forces are plotted as a function of interparticle distance at a contact angle of 45 deg, are similar to those in Figure 3 (θ = 0 deg) except that the magnitude of capillary forces is smaller (less attractive). The situation is very different when capillary forces are calculated for a contact angle of 85 deg. The results of the calculation are shown in Figure 10. The capillary forces are negative (repulsive) for a small interparticle distance. As the distance increases, the curves of the capillary force pass through zero and become attractive for large values of D. At an interparticle distance of D_e the system is at equilibrium. If the system departs from D_e, it will return to the equilibrium position eventually.

Mason and Clark[20] found that the geometry of the liquid bridge must be a portion of a sphere when the force is zero

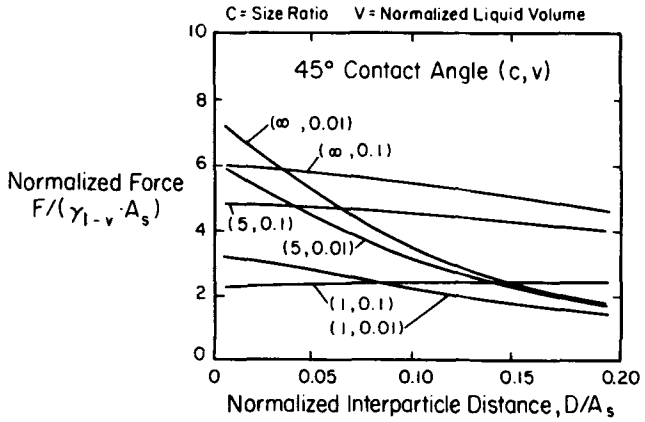

Fig. 9—The capillary force acting between two spheres or a sphere and a plate connected by a liquid bridge as a function of the normalized interparticle distance for a contact angle θ = 45 deg, and the size ratios C = 1, 5, and ∞.

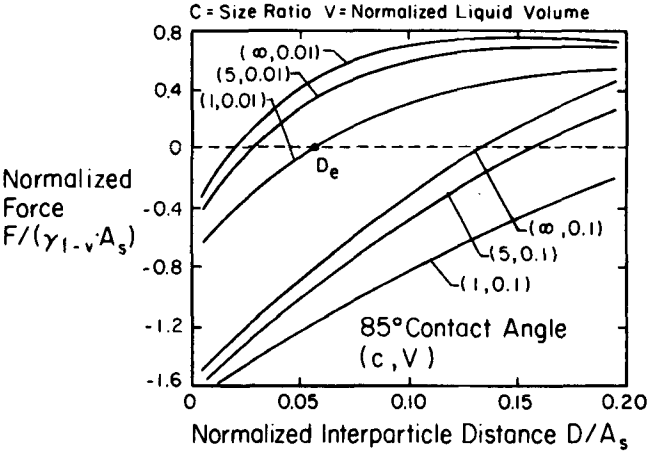

Fig. 10—The capillary force acting between two spheres or a sphere and a plate connected by a liquid bridge as a function of the normalized interparticle distance for a contact angle θ = 85 deg, and size ratios C = 1, 5, and ∞.

at $D = 0$. The current calculations show that even when the spheres are separated by a distance, the liquid profile is still spherical for the zero capillary force condition.

The values of the contact angle when the capillary force is zero at zero interparticle separation ($D = 0$) were calculated for different amounts of liquid and various size ratios of the spheres. The results are shown in Figure 11. The critical contact angle for zero force decreases with increasing volume. For each of the three curves for different size ratios ($C = 1, 5, \infty$) the region below the curve is the one where an attractive force is exerted while above the curve the force is repulsive and the spheres will be pushed apart. Contact angles of real materials are usually smaller than the critical values plotted in Figure 11, so that shrinkage or agglomeration of loose powders due to the attractive capillary force is expected.

V. DISCUSSION

Since the results include small numerical errors, they were compared with the available analytical solutions to assess their validity. For two contacting spheres the analytical solution which includes incomplete elliptical integrals was first found by Fisher.[11] A comparison of capillary forces at twelve liquid volumes shows Fisher's results and our numerical solutions agree within 0.1 pct or better for all cases.

In addition to the above comparison, three other checks were made by simple analytical solutions for the capillary forces which are possible for particular geometries. They occur when the pressure deficiency P in Eq. [3] is equal to 0, γ_{l-v}/H, and $2\gamma_{l-v}/H$ where H is the liquid neck radius as shown in Figure 1.

For $P = 0$, the meridian curve is called catenoid and is described by a hyperbolic cosine function. For $P = \gamma_{l-v}/H$, the geometry is a cylindrical profile which occurs when the liquid-vapor interface is parallel to the x-axis. The third geometry occurs when the liquid bridge is part of a sphere. This configuration satisfies Eq. [3], because the two principal radii are both equal to H and the pressure deficiency is therefore equal to $2\gamma_{l-v}/H$ at any point along the liquid-vapor interface.

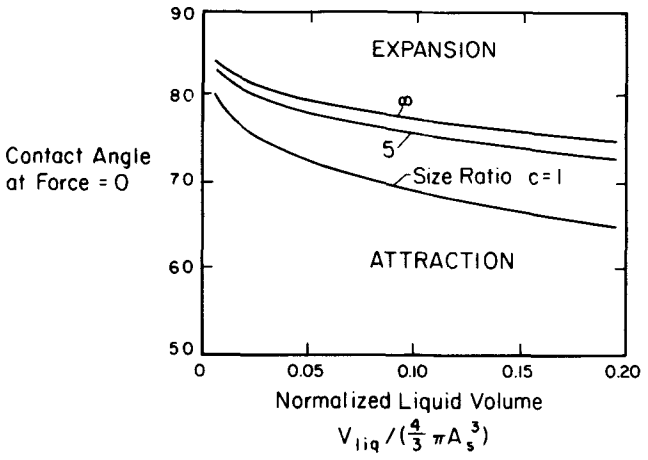

Fig. 11 — The critical contact angle (in degrees) for zero capillary force as a function of the liquid volume for three size ratios $C = 1$, 5, and ∞.

To compare the results calculated by the numerical method with the three geometries, the volumes of the liquid bridge based on the geometries were first calculated analytically. From the same liquid volume and the same system variables (D, θ, C), the coordinates of the liquid profile of the system were calculated. The coordinates of the liquid profile were compared with the function representing each of the three particular geometries, *i.e.*, catenoid, cylinder, and sphere. In all three cases, no difference on the profile between the two results was found. Based on these checks, it is reasonable to say that the numerical method and the computer program written for it are correct.

Results of capillary forces calculated numerically for two systems consisting of identical spheres ($C = 1$) and a sphere and a plate ($C = \infty$) can be compared with experimental results reported by Mason and Clark[19] (Figures 12 and 13). In Figure 12, the theoretical calculations of capillary forces at three different liquid volumes for the system consisting of two identical spheres are drawn in solid lines. The calculated values agree fairly well with the experi-

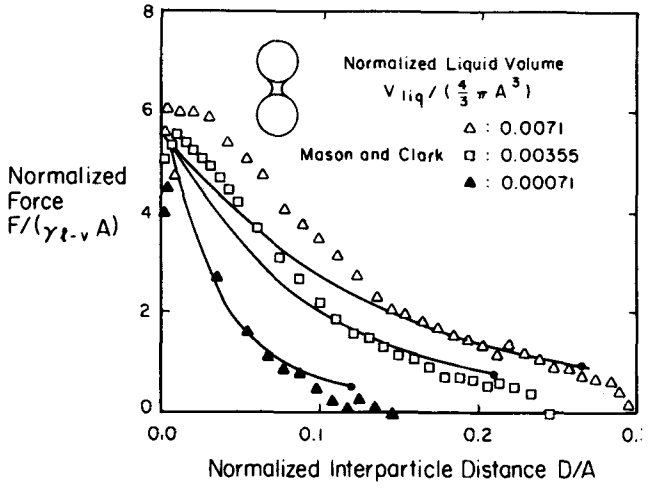

Fig. 12 — A comparison between experimental data measured by Mason and Clark and theoretical calculations obtained from this study on capillary forces for a system consisting of two identical spheres with a contact angle $\theta = 0$ deg.

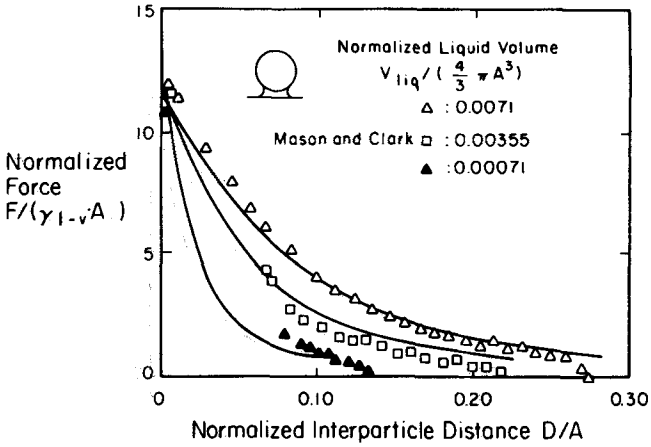

Fig. 13 — Comparison of experimental data measured by Mason and Clark and theoretical calculations obtained from this study on capillary forces for a system consisting of a sphere and a plate with a contact angle $\theta = 0$ deg.

mental results except when the liquid volume equals 0.0071. In Figure 13, the theoretical calculations agree with the experimental results for all three liquid volumes for the system consisting of a sphere and a plate.

Some past investigations of the capillary force have used an approximate force calculation based on a circular profile for the liquid bridge. In this case the pressure inside the liquid is not homogeneous. The errors introduced by using this approximation instead of the numerical solutions based on the nodoid profile were calculated for a wide range of contact angles, interparticle distances, liquid volumes, and particle sizes. In Figure 14 the percentage error of the approximate method is plotted as a function of the interparticle distance for various liquid volumes and contact angles for a system consisting of identical spheres. Note that the dashed line represents zero error. In the case of a small contact angle ($\theta = 0$ deg), the percentage error at $D = 0$ is greater than 5 pct. As the interparticle distance increases, the error of the approximate method increases. Also the percentage error of the approximate method depends on the liquid volume. As the liquid volume decreases, the discrepancy between the results from the approximate method and the numerical method increases, especially when the interparticle distance is large. It was also found that as contact angles increased, the percentage error decreased. For spheres of different sizes, the errors generally increase as the particle size ratio C increases.

From the above examination it is seen that the approximate method is not reliable for small contact angles, low liquid volumes, large particle size differences, and large interparticle distances. For this reason the force method has led to wrong conclusions with regard to capillary forces[17,18] under such conditions. For example, Smolej and Pejovnik[17] used the approximate method to calculate the capillary force for low contact angles, large interparticle distances, and small liquid volumes. Their data are shown in Figure 15 as dashed lines, indicating a metastable equilibrium at point D_u where the capillary force is zero. However, no such metastable equilibrium exists when the capillary forces are calculated using the nodoid profile. The curves calculated in this study are shown as solid lines in Figure 15. The circled points indicate the calculated conditions for which rupture is expected to occur. This indicates that the capillary force never reaches zero or a negative value before rupture.

Finally, a comparison can be made between the capillary force and the weight of the sphere. As an example, the case of two identical spheres connected by a liquid bridge with a normalized volume $V = 0.01$ and the contact angle $\theta = 8$ deg is studied. The capillary force exerted on the sphere is $4.94A\gamma_{l-v}$ at $D = 0.01A$ and $0.97A\gamma_{l-v}$ at rupture, where A is the radius of the sphere and γ_{l-v} is the surface tension of the liquid. If $\gamma_{l-v} = 1$ N/m, $A = 10$ μm and the density of the sphere $\rho = 10$ g/cm^3, then the capillary force exerted on the sphere is about 10^5 and 2×10^4 times that of its own weight at $D = 0.1$ μm and at rupture, respectively. Thus, if spheres are connected by a liquid bridge, they will be pulled toward each other by this large capillary force, and the time of the movement should be very short. Accordingly, the short period needed for particle agglomeration (such as in spray drying) and rearrangement in liquid phase sintering seems reasonable in light of the relatively large forces calculated for a wetting liquid.

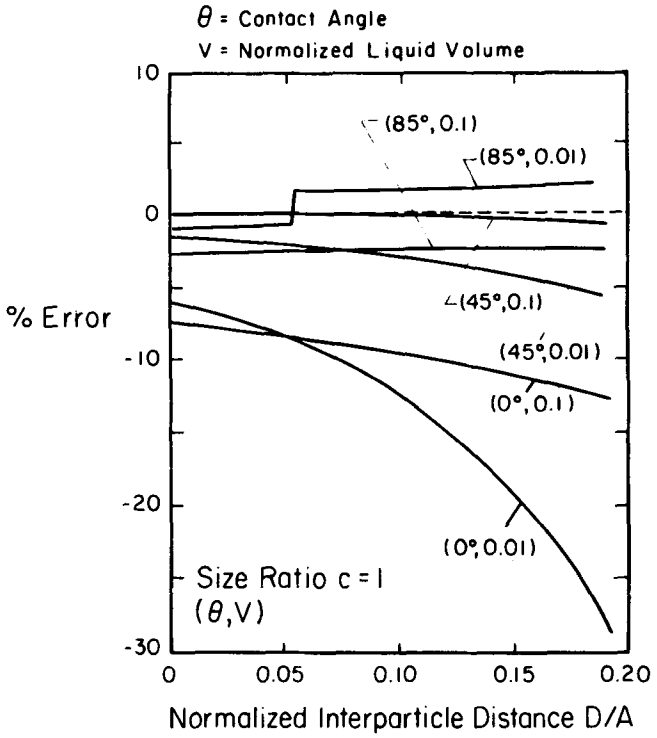

Fig. 14—The percentage error of the capillary force calculated by the approximate method as a function of the interparticle distance for a system consisting of identical spheres ($C = 1$).

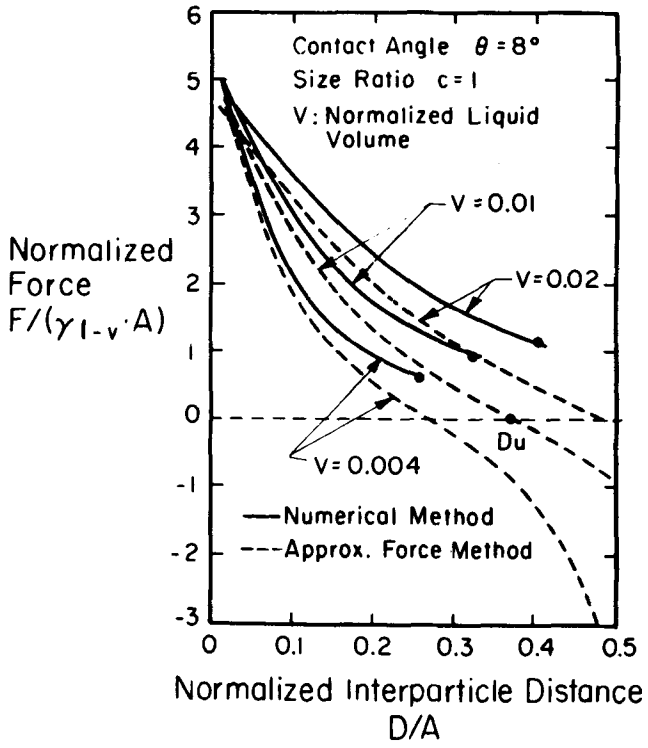

Fig. 15—The capillary forces calculated by the approximate method and by the numerical method as a function of the interparticle distance for a system consisting of two identical spheres with a contact angle $\theta = 8$ deg.

VI. CONCLUSIONS

The calculation of capillary forces has been performed using a numerical method based on a nodoid profile. A wide range of system variables, *i.e.*, interparticle distance D, contact angle θ, liquid volume V, and particle size ratio C, is considered in this study. The effect of each variable on the capillary force has been discussed. A large capillary force is associated with a small separation distance between the spheres, a small contact angle, and uniform distribution of the liquid. At small contact angles rupture can occur even when the capillary force is attractive. The critical condition for rupture is calculated from the free energy of the system. At large contact angles a zero force condition exists for which the system is at an equilibrium separation between spheres. When the calculation is based on a circular liquid profile, the errors are small only for large liquid volumes, large contact angles, and small interparticle distances.

ACKNOWLEDGMENTS

This paper resulted from the Ph.D. thesis of K.S. Hwang who was supported by Remington Arms and Allegheny Ludlum Steel during his studies at Rensselaer Polytechnic Institute. Professor German was supported by the United States Department of Energy.

REFERENCES

1. R.M. German: *Liquid Phase Sintering*, Plenum Press, New York, NY, 1985.
2. K.L. Wardle: *Differential Geometry*, Dover Publications, New York, NY, 1965, p. 5.
3. N.L. Cross and R.G. Picknett: *International Conference on Mechanism of Corrosion by Fuel Impurities*, Marchwood Eng. Lab., England, 1963, pp. 383-90.
4. K. Hotta, K. Takeda, and K. Ilnoya: *Powder Tech.*, 1974, vol. 10, pp. 231-42.
5. T. Gillespie and W.J. Settineri: *J. Colloid Interface Sci.*, 1967, vol. 24, pp. 199-202.
6. R.B. Heady and J.W. Cahn: *Metall. Trans.*, 1970, vol. 1, pp. 185-89.
7. H. Schubert: *Chemie-Ing.-Techn.*, 1968, vol. 40, pp. 745-47.
8. H. Emi, S. Endo, C. Kanaoka, and S. Kawai: *Int. Chem. Eng.*, 1979, vol. 19, pp. 300-06.
9. B. Derjaguin: *J. Colloid Interface Sci.*, 1968, vol. 26, pp. 253-53.
10. H.M. Princen: *J. Colloid Interface Sci.*, 1968, vol. 26, pp. 249-53.
11. R.A. Fisher: *J. Agri. Sci.*, 1926, vol. 16, pp. 492-505.
12. L.V. Radushkevich: *Akad. Nauk SSSR, Izvestia. Seriia Khimicheskaia*, 1952, pp. 1008-18.
13. J.C. Melrose: *A.I.Ch.E. Journal*, 1966, vol. 12, pp. 986-94.
14. L.V. Radushkevich: *Akad. Nauk SSSR, Izvestia. Seriia Khimicheskaia*, 1958, pp. 403-10.
15. H. Rumpf: *Chemie-Ing.-Techn.*, 1974, vol. 46, pp. 1-11.
16. K.S. Hwang: Ph.D. Thesis, Rensselaer Polytechnic Institute, Troy, NY, May 1984.
17. V. Smolej and S. Pejovnik: *Z. Metallkde.*, 1976, vol. 67, pp. 603-05.
18. W. Pietsch and H. Rumpf: *Chemie-Ing.-Techn.*, 1967, vol. 39, pp. 885-93.
19. G. Mason and W.C. Clark: *Chem. Eng. Sci.*, 1965, vol. 20, pp. 859-66.
20. G. Mason and W. Clark: *British Chem. Eng.*, 1965, vol. 10, pp. 327-28.